Diffusion of a Single Component in a Binary Polymer Blend upon Annealing Monitored by Fluorescence Microspectroscopy

Marcelo L. de Andrade and Teresa D. Z. Atvars*

Instituto de Química, Universidade Estadual de Campinas, Campinas, São Paulo, Brazil

Received June 8, 2004; Revised Manuscript Received August 19, 2004

ABSTRACT: We describe the employment of steady-state fluorescence spectroscopy coupled to epifluorescence microscopy (fluorescence microspectroscopy) for monitoring the diffusion of the lower-T_g component during heating of a binary blend of poly(*n*-butyl methacrylate-*co*-styrene) containing 9-vinylanthracene units attached as fluorescent label (nBMAS) with polystyrene. The segregation of the nBMAS was monitored by simply measuring the emission spectra over areas of a few micrometers at 40 °C (above nBMAS-T_g) near the interfacial region as a function of time, while the morphological changes and the flux of diffusant were readily revealed during the annealing process. The apparent diffusion coefficient, $D_{ap} = (1.6 \pm 0.1) \times 10^{-6}$ cm^2 s^{-1}, was extracted from the slope of the better linear fitting from the plot of relative intensities (as integrated spectra) vs $t^{1/2}$.

Introduction

The diffusion of the components in miscible or immiscible binary polymer blends has been the subject of many investigations and is of scientific and technological interest for several applications because it influences important properties such as adhesion, wetting, and friction. During the annealing of a polymer blend above the glass transition temperature of a single or both components, a significant segregation of the polymer chains arises as a result of the differences of the surface energy between the components and of the small combinatorial entropy of mixing and leads to significant compositional changes on the time scale of minutes.[1]

Measurement of diffusion coefficients requires the determination of the concentration profile for the diffusant as a function of time. In recent years several methods with different spatial resolutions have been developed to measure the concentration profile at polymer−polymer interfaces and polymer surfaces, including forward recoil spectrometry (FRS),[2] nuclear reaction analysis (NRA),[3] neutron reflectometry (NR),[4] positron annihilation lifetime spectroscopy (PALS),[5] secondary ion mass spectroscopy (SIMS),[6] and fluorescence electron spectroscopy (FES).[7] Unfortunately, none of these techniques allow visualizing the course of the diffusant, and hence they do not reveal the morphology during the segregation process.

In this paper, we present an attractive alternative method for studying and measuring diffusion in polymer blends during annealing, employing the fluorescence microspectroscopy (FMS) and epifluorescence optical microscopy (EFIM). Although this approach have been already used by some researchers to investigate the diffusion of small molecules (additives) in polymer matrices,[8] to our knowledge this paper is the first attempt to apply this technique to study the diffusion of a macromolecular component in polymer blends during annealing. Here the system is a blend of 50 wt % of poly(*n*-butyl methacrylate-*co*-styrene) (nBMAS), labeled with 9-vinylanthracene (9-VAn), moieties, and polystyrene (PS), already characterized as a system with phase separation produced by the mechanism of nucleation and growth.[9]

* Corresponding author: Fax 55-19-37883023; Tel 55-19-37883078; e-mail tatvars@iqm.unicamp.br.

Experimental Section

The synthesis and the characterization of the anthracene-labeled copolymer nBMAS examined here have been previously reported.[9] Commercial PS (EDN-Brazil) with a number-averaged molecular weight of 64 kg/mol (polydispersity 2.6) was used without further purification. Chloroform used here was of analytical grade (Merck). The film of a nBMAS/PS blend with 50 wt % (approximate thickness of 0.3 mm) was prepared by casting 10% chloroform solutions on a silanized Petri dish (to avoid adhesion). The solvent was slowly evaporated (2 days at room temperature), and then the films were dried for a day under dynamic vacuum. The film thickness is ∼300 μm.

Dynamic-mechanical thermal analysis (DMTA) of the neat components and the blend were carried out by means of a Thermal Analyst 2100-DMA 983 (TA Instruments) at a frequency of 1 Hz from −100 to 200 °C. Samples of dimensions ca. 9.0 × 4.0 × 0.3 mm were previously annealed at 100 °C for 10 h and then submitted to sinusoidal deformation with 0.20 mm amplitude. The samples were heated in steps of 3 °C, remaining at each temperature for enough time to reach thermal equilibrium.

Steady-state fluorescence microspectroscopy (FMS) was performed using a ISS-PC1 spectrofluorimeter which has been adapted to be coupled to a Leica DM IRB epifluorescence microscope. An external 5 cm optical lens focuses the microscopic image on the entrance of the optical fiber, which directs the optical signal to the focus point of the sample housing within the fluorimeter. This optical fiber has been inserted into the lateral exit of the microscope. Small slices of sample (∼1 cm diameter, 300 μm thickness) were mounted between two glass windows spaced by an aluminum ring in the hot stage (Linkam THMS 600) equipped with a temperature controller (Linkam TMS 94). Because of the spacer, the sample is confined between the windows, and no mass loss was possible during the experiment. The sample was heated slowly to a temperature of 30 °C above the nBMAS glass transition temperature and then heated at a rate of 6 °C/min from 60 to 110 °C. The temperature was held constant for 3 min for each increment step of 10 °C, while the emission spectrum and the epifluorescence image were simultaneously obtained. The excitation of 9-anthryl moieties took place by employing the HBO (HBO-100 W) mercury arc lamp of the microscope whose wavelength range was selected as 330−380 nm by an optical filter. The epifluorescence image was separated from the

10.1021/ma048873r CCC: $27.50
Published on Web 11/09/2004

Table 1. Physical Properties of nBMAS and PS Polymers

polymer	T_g (°C)[a]	$\bar{M}_n$ (kg/mol)[b]	$\bar{M}_w/\bar{M}_n$	nBMA (mol %)[c]	STY (mol %)[c]	9-VAn (mol %)[c]
nBMAS	37	31.2	2.7	77.5	22.4	0.1
PS	95	64.6	2.58	0	100	0

[a] These T_g values was taken from the maximum of the peaks in the log(tan δ) × T traces by DMTA measurements. In a previous work,[9] T_g values were determined by DSC measurements, giving 22 and 91 °C for nBMAS and PS, respectively. [b] Obtained from GPC. [c] Obtained from UV−vis.

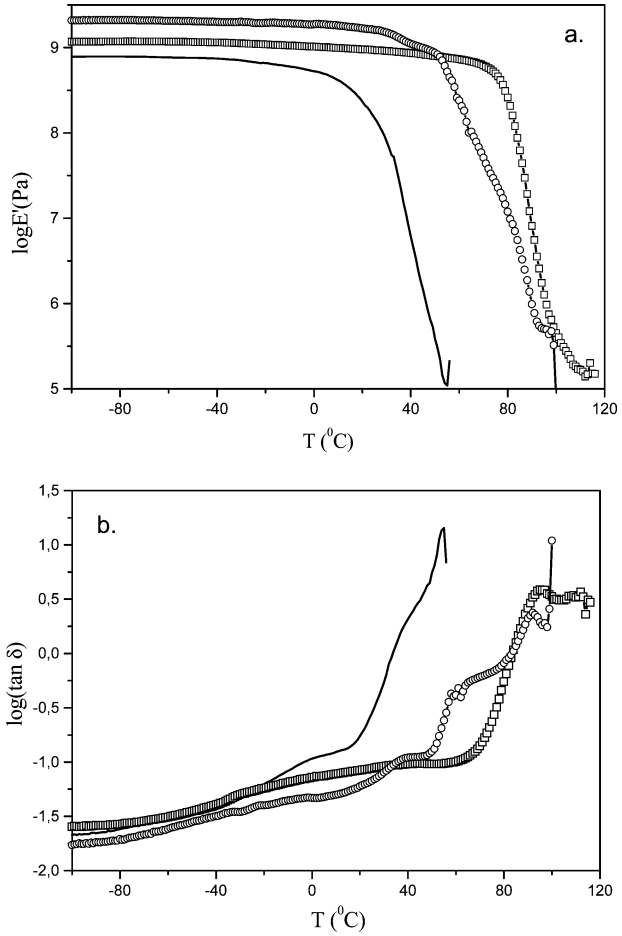

Figure 1. DMA traces (1 Hz, 3 °C/min) for nBMAS (—), PS (□), and the nBMAS/PS blend with 50 wt % (○): (a) storage modulus (E') vs temperature and (b) loss tangent [log(tan δ)] vs temperature.

excitation beam by a dichroic mirror (λ_{exc} > 410 nm). Objective magnifications of 50×, 200×, and 630× (to obtain areas as small as few micrometers) were used, and the images were taken with a Samsung SDC-311 digital camera and processed with a Linksys v. 2.38 software. Photomicrographs were obtained using the epifluorescence configuration. Blue regions from the images are due to the fluorescence from anthryl-labeled copolymer (nBMAS). Fluorescence spectra of the respective images were recorded in the range 410−550 nm.

Results and Discussion

Some physical properties of the neat components (nBMAS and PS) are shown in Table 1. Characterization of the copolymer composition, molecular weight, and molecular weight distribution, as well as other physical-chemical and thermochemical properties, have been published elsewhere.[9] The curves of storage modulus (E') and (tan δ) loss tangent as a function of the temperature for the neat components (nBMAS and PS)

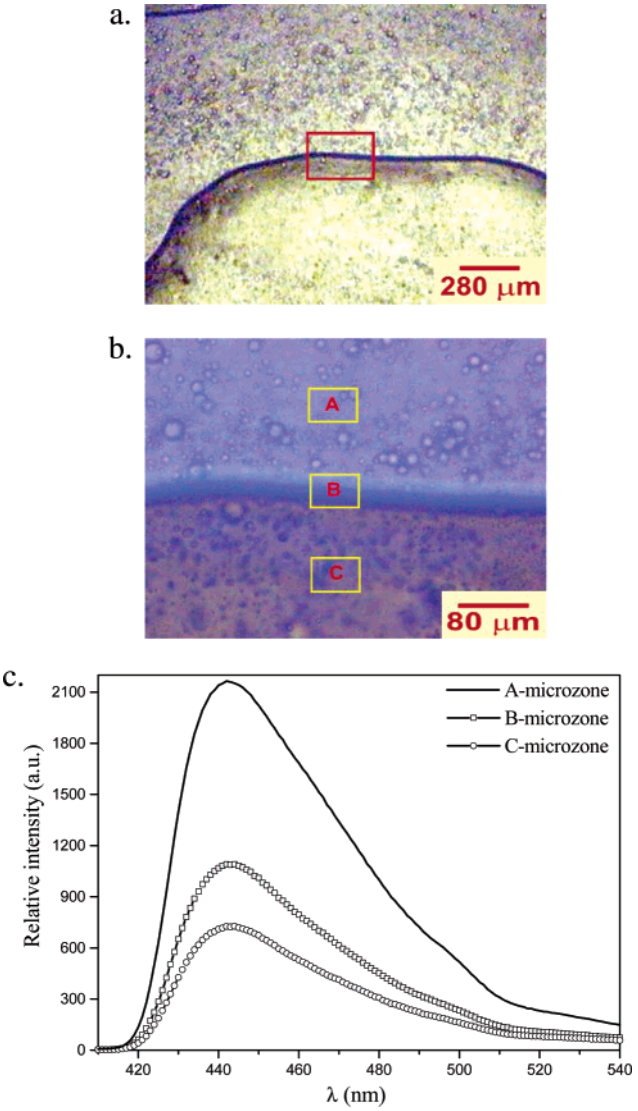

Figure 2. (a) EFM micrograph of nBMAS/PS blend with 50 wt % of copolymer after annealing. (b) Further magnification of the nBMAS/PS blend showing the interface between the matrix richer in nBMAS (blue emission from the 9-anthryl moieties) and the PS-rich large droplets (nonfluorescent). (c) Fluorescence microspectra of the three regions specified in micrograph b.

and for the symmetric composition blend (50 wt %) are shown in Figure 1. The temperatures corresponding to the maximum of the peaks in the log(tan δ) curves are assigned to the relaxation temperatures: glass transition (T_g) or secondary relaxation (T_s).[9]

The T_g values for the neat components are shown in Table 1. According to the DMTA traces of Figure 1, the nBMAS/PS blend with 50 wt % presents three T_g values: one at 40 °C, near the T_g of the neat nBMAS copolymer, another at 92 °C, near the neat PS, and another at 63 °C, showing that miscibility with PS occurred in the nBMAS-richer matrix, as also shown by the epifluorescence image in Figure 2a. In these images the blue-fluorescent domains contain copolymer labeled with anthryl groups and some amount of PS, while the nonfluorescence domains are composed of polystyrene.

The microfluorescence spectra depicted in Figure 2b,c support the arguments mentioned above. As we can see in Figure 2a, the 50 wt % nBMAS/PS blend is composed of large PS-richer droplets of several shapes and sizes, varying from more perfectly spherical to deformed

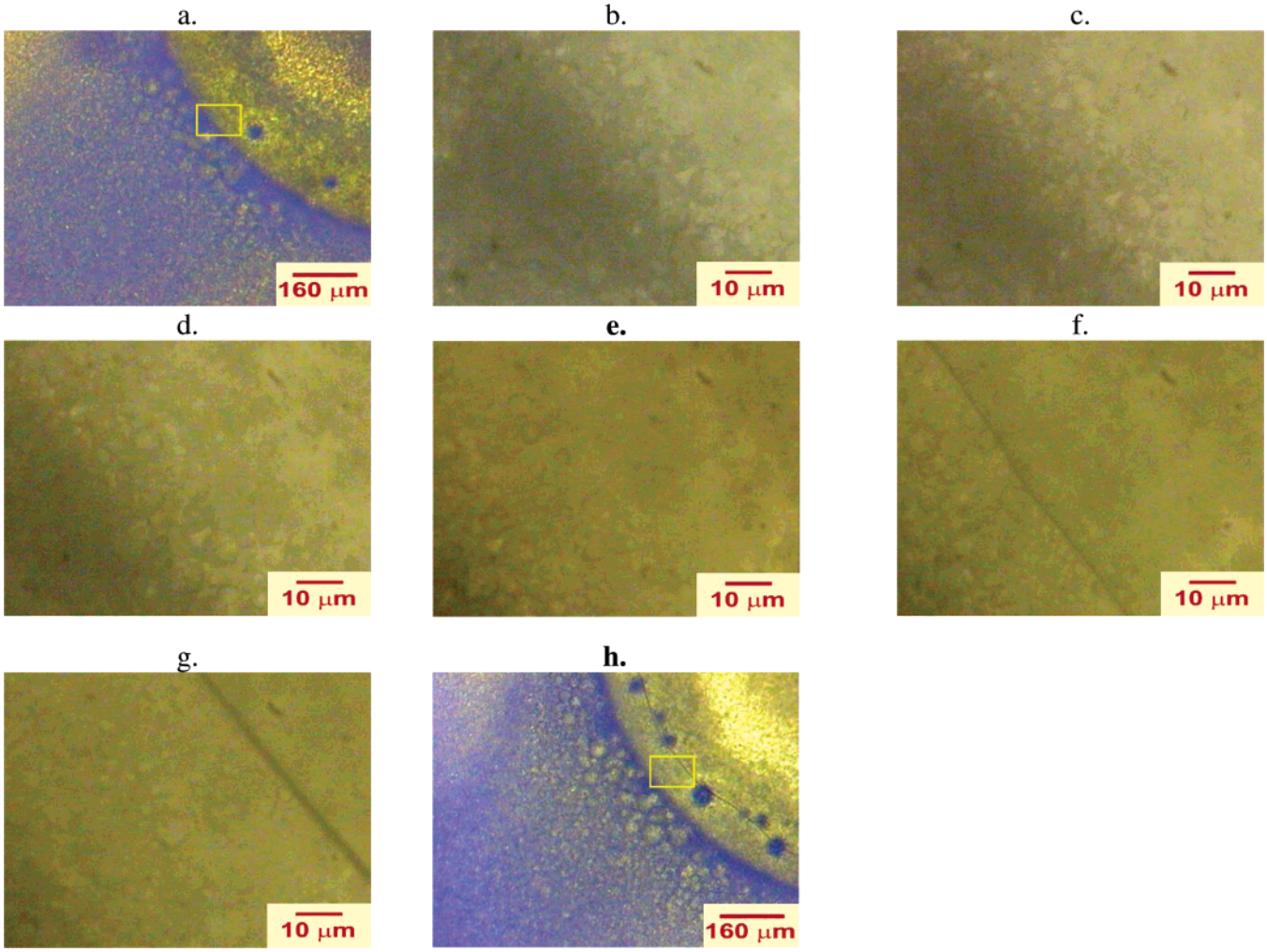

Figure 3. EFM micrographs of a nBMAS/PS blend sample with 50 wt % component in the course of the annealing process: (a) before annealing at 40 °C; (b−g) magnifications of the zone depicted in (a) after 0 (40 °C) (a), 20 (40 °C) (b), 36 (50 °C) (c), 76 (70 °C) (d), 92 (90 °C) (e), and 115 min (100 °C) (f); (h) EFM of the final morphology after 28 min at 40 °C.

droplets over an intense fluorescent nBMAS-richer matrix. Besides this, a bright ring around the droplets is clearly seen, which behaves as a highly emissive interface, although it is often described as an exclusion zone.[10] Figure 2b shows a magnification of the area depicted in Figure 2a that includes an interface. In this picture we identify three microzones labeled as A, B, and C whose fluorescence spectra are depicted in Figure 2c. Microzone A exhibits the high emission intensity of the 9-anthryl moieties and can be identified as a nBMAS-richer phase. Microzone B contains the interface, and it is also strongly fluorescent. Microzone C is less fluorescent, being formed by a PS-richer phase (microzone C). Therefore, the fluorescence intensity is an approximated measurement of the phase composition if scattered emission is neglected, and this system can be described as biphasic, composed by two phases with distinct compositions connected by an interface.

Figure 3a shows the initial morphology (before annealing) of the 50 wt % nBMAS/PS blend film, which was further submitted to heating from 40 °C (above the T_g of the nBMAS copolymer) to 100 °C (above the T_g of the PS), step by step. At every temperature an image (Figure 3b−g) was recorded. These images contain the interface, and because of mass diffusion, the interface is displaced and becomes thinner, if compared with the initial sample (Figure 3a). The morphological changes near the interface (enlarged images in Figure 3b−g) result from the segregation of the component with lower T_g value (nBMAS, T_g = 37 °C) as also seen by visual inspection of the micrographs by following the displacement of the darker stain (blue fluorescent contrast appears slightly changed at higher magnification) toward the outside of the droplets. Hence, the diffusion of the fluorescent material (nBMAS) can be followed by changes of the color of the PS-richer phase from soft green to strong yellow under illumination with a mercury lamp filtered by the 330−380 nm excitation optical filter and the λ_{exc} > 410 nm dichroic mirror. In addition, we also observe that near the PS T_g (90 °C) the nonfluorescent material starts flowing, as can be seen in the micrographs in Figure 3f,g. Finally, the morphology after annealing is composed of a thinner interface and larger PS-richer droplets, as shown in Figure 3f,g. The displacement of the interface in relation to its original position (Figure 3a) is a consequence of the enlargement of the droplets. Thus, in addition to the enhancement of the phase separation process, the annealing process also produce thinner interface between the matrix and the droplets. However, as seen by comparison with Figure 3a, the shift of the interface was significant only at temperatures higher than 90 °C. Thus, the interface could be assumed to be stationary during the characteristic segregation of the nBMAS

below the PS glass transition temperature. Therefore, at higher temperatures (near or above both glass transition temperatures) the net diffusional flux of each component can be determined by the summation of the fractional fluxes. Because of the distinct molecular weights, the net fluxes, in general, will not match each other. Experimentally, convective flow reveals itself by movement of the interface toward the faster diffusing component.[11]

Assuming that the fluorescence intensity is proportional to the amount of anthryl moieties in the phase, which is itself proportional to the nBMAS copolymer composition, any change of the phase composition produced by one-component net diffusion can be correlated with the fluorescence intensity. Thus, when the lower-T_g component diffuses through the interface from the PS-richer domains, this zone is depleted in that component and its fluorescence should decrease. Although the diffusion is a three-dimensional process and the fluorescence intensity is a collection of the total emission that arises from the entire probed zone, the most important observation here is the displacement of the interface. Under such circumstances the amount of the segregated material should be controlled by the diffusion distance, $(D_{ap}t)^{1/2}$, where D_{ap} is the "apparent" diffusion coefficient, which accounts for the segregation process and t is the annealing time. Here we are assuming that because PS-T_g is much higher than nBMAS-T_g, the segregation takes place only by the diffusion of the nBMAS copolymer when the experimental temperature is $T < T_{g,PS}$. Because the nBMAS copolymer is excluded from the PS droplets, we assume that the maximum diffusional distance (l_{max}) is equal to the maximum diameter (0.9 mm) of the PS-richer domains. Thus, the apparent diffusion coefficient (D_{ap}) for the interfacial segregation of the nBMAS copolymer can be evaluated by measuring the fluorescence intensities during the annealing at constant temperature by employing eq 1, derived from the second Flick's law:[12]

$$(I_0 - I_t)/(I_0 - I_\infty) = (4/l_{max})(D_{ap}/\pi)^{1/2}t^{1/2} \qquad (1)$$

where I_0 is the fluorescence intensity from 9-anthryl groups at time = 0, I_t is the fluorescence intensity from 9-antryl groups after t seconds of annealing, at the temperature of the experiment, and I_∞ is the fluorescence intensity from 9-anthryl groups over the maximum time of annealing at the same temperature. These values of intensity were taken as the integrals of the fluorescence spectra.

Here the fluorescence intensity of the 9-anthryl groups of the 50 wt % nBMAS/PS blend at 40 °C was measured, collecting spectra at constant time intervals from the initial time ($t = 0$) to $t = 28$ min (Figure 4a). Using eq 1, the $D_{ap} = (1.6 \pm 0.1) \times 10^{-6}$ cm^2 s^{-1} was evaluated from the slope of the best linear fit over the range $0.1 \le (I_0 - I_t)/(I_0 - I_\infty) \le 1.0$ (Figure 4b). Reproducibility was already tested in different parts of the same sample. However, because of the difference of composition in these different zones, we do not reproduce the same value for the ratio $(I_0 - I_t)/(I_0 - I_\infty)$ at one specific time. Nevertheless, the curve profile is almost parallel to that showed in Figure 4b.

According to the literature, values of diffusion coefficients ranged from 10^{-5} to 10^{-15} cm^2 s^{-1} have been reported, depending on the system, the composition, and the temperature.[13] For example, apparent diffusion

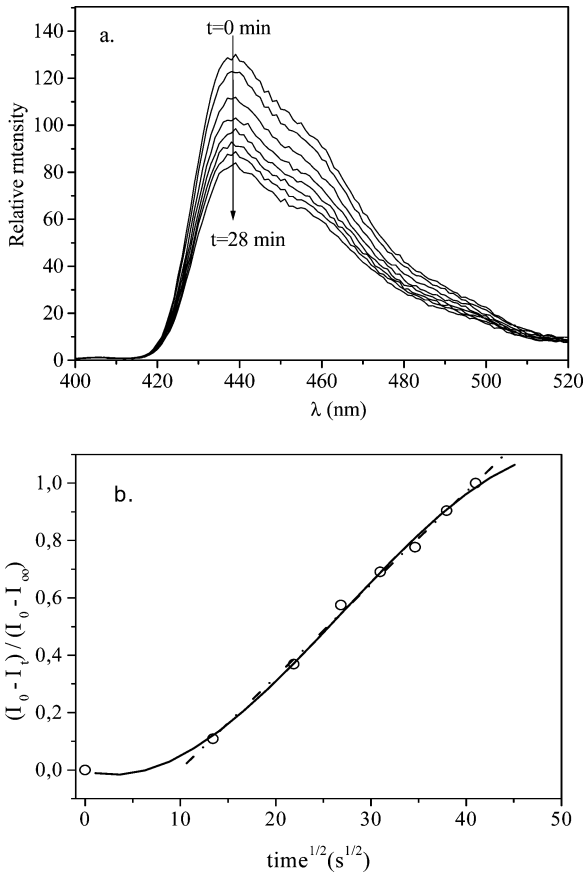

Figure 4. (a) Fluorescence microspectra at 40 °C (from $t = 0$ to $t = 28$ min); (b) circles are he experimental data. Solid line: Flick's law plot of the data obtained from spectra of (a). Dashed line: best linear fit (angular coefficient = 0.0322 and linear correlation = 0.9985) of the data along the ordinate between 0.1 and 1.0.

coefficients varying between 10^{-11} and 10^{-9} cm^2 s^{-1} (at several temperatures) have been reported for polydisperse high-density polyethylene (HDPE) and linear low-density polyethylene (LLDPE) as microlayers.[1] The surface segregation in annealed blends of random copolymers of styrene and acrylonitrile (SAN) with different acrylonitrile contents resulted in apparent diffusion coefficients of ca. 10^{-15} cm^2 s^{-1}.[14] Diffusion coefficients of the blend of the two thermodynamically miscible polymers, poly(vinyl chloride) (PVC) and poly(*n*-butyl methacrylate) (PnBMA), during annealing at temperatures above the T_g of both polymers have been determined as 10^{-13}–10^{-14} cm^2 s^{-1}.[5] All of these values are lower than those determined here, for nBMAS/PS at 50 wt % and 40 °C, and unfortunately other data under our experimental conditions are not available. However, apparent diffusion coefficients from $(4.3 \pm 1.9) \times 10^{-6}$ to $(4.0 \pm 1.0) \times 10^{-5}$ cm^2 s^{-1} have been reported for the segregation of diblock poly(styrene-*b*-dimethylsiloxane) [P(S-*b*-DMS)] copolymers added to a molten blend of the corresponding immiscible homopolymers,[15] and these are quite similar to our data. So far, straightforward comparisons cannot be made because either the systems or experimental conditions are different.

To use such an approach, we must be sure that the only effect responsible for the decrease of the fluorescence intensity is the diffusion of the fluorescent component out of the phase probed by the microscope. Photobleaching of the fluorophore in the microscope focus is one problem to be avoided, and several types of

approaches have been employed to prevent photobleaching.[16,17] Fortunately, this is not the case here, as seen by comparing parts a and h of Figure 3: in these figures the color of the images is virtually the same out of the droplets, including at the interface, and the major difference is displacement of the interface toward the matrix, as seen by the position of the rectangle (area $\approx$ 0.007 mm^2) in a fixed position. If photobleaching played an important role, the entire region would be bleached.

Conclusions

We have successfully employed steady-state fluorescence spectroscopy and epifluorescence optical microscopy for monitoring individual diffusion of the lower-T_g component of the 50 wt % nBMAS/PS blend during annealing. Simultaneous epifluorescence images and fluorescence spectra of the same image zone can be recorded by coupling both instruments. Hence, we can simultaneously follow the morphological changes and emission spectra as the annealing process takes place. Epifluorescence images demonstrated that, under annealing, there is a morphological change enlarging the size of the PS droplets in the nBMAS matrix in addition to a remarkable decrease of the interface thickness. Because the only fluorescence species is the copolymer, under our experimental conditions, photobleaching does not occur and the fluorescence intensity is a measure of the copolymer composition in the phase. Thus, by measuring changes of the fluorescence intensity at a constant temperature, we were able to determine the apparent diffusion coefficient of the nBMAS out of the PS-richer phase when the temperature is lower than the PS glass transition. The value at 40 °C is $(1.6 \pm 0.1) \times 10^{-6}$ cm^2 s^{-1}.

This technique also shows some additional advantages: (i) no further preparation of the sample is required, (ii) measurements can be performed using small samples and short time intervals, (iii) the experiment can be carried out at any temperature using a proper heating stage in the microscope, and (iv) no other component is required such as a solvent.

Acknowledgment. T.D.Z.A. and M.L.A. thank FAPESP, CNPq, FAEP/UNICAMP, and MCT/PADCT/IMMP for financial support and fellowship. The authors thank Prof. Carol Collins for useful discussions.

References and Notes

(1) Green, P. F. Translational Dynamics of Macromolecules in Melts. In *Diffusion in Polymers;* Neogi, P., Ed.; Marcel Dekker: New York, 1996.
(2) . (a) Genzer, J.; Composto, R. J. *Macromolecules* **1998**, *31*, 870. (b) Kim, E.; Kramer, E. J.; Garrett, P. D.; Mendelson, R. A.; Wu, W. C. *Polymer* **1995**, *36*, 2427.
(3) (a) Budkowski, A.; Losch, A.; Klein, J. *Isr. J. Chem.* **1995**, *35*, 55. (b) Chaturvedi, U. K.; Steiner, U.; Zak, O.; Krausch, G.; Klein, J. *Phys. Rev. Lett.* **1989**, *63*, 616. (c) Chaturvedi, U. K.; Steiner, U.; Zak, O.; Krausch, G.; Schatz, G.; Klein, J. *Appl. Phys. Lett.* **1990**, *56*, 1228.
(4) Geoghegan, M.; Nicolai, T.; Penfold, J.; Jones, R. A. L. *Macromolecules* **1997**, *30*, 4220.
(5) (a) Dlubek, G.; Pionteck, J.; Bondarenko, V.; Pompe, G.; Taesler, C.; Petters, K.; Krause-Rehberg, R. *Macromolecules* **2002**, *35*, 6313. (b) Dlubek, G.; Bondarenko, V.; Pionteck, J.; Kilburn, D.; Pompe, G.; Taesler, C.; Redmann, F.; Petters, K.; Krause-Rehberg, R.; Alam, M. A. *Radiat. Phys. Chem.* **2003**, *68*, 369.
(6) Brown, H. R.; Char, K.; Deline, V. R. *Macromolecules* **1990**, *23*, 3383.
(7) (a) Pekcan, Ö.; Canpolat, M.; Göçmen, A. *Polymer* **1993**, *34*, 3319. (b) Deppe, D. D.; Dhinojwala, A.; Torkelson, J. M. *Macromolecules* **1996**, *29*, 3898.
(8) (a) Billingham, N. C.; Calvert, P. D. *Pure Appl. Chem.* **1985**, *57*, 1727. (b) Johnson, M.; Westlake, J. F. *J. Appl. Polym. Sci.* **1975**, *19*, 1745.
(9) de Andrade, M. L.; Atvars, T. D. Z. *J. Phys. Chem. B* **2004**, *108*, 3975.
(10) (a) Cruz, M. C. P.; Cassiola, F. M.; Atvars, T. D. Z. *J. Appl. Polym. Sci.* **2002**, *84*, 1637. (b) Dibbern-Brunelli, D.; Atvars, T. D. Z. *J. Appl. Polym. Sci.* **1995**, *58*, 779. (c) Dibbern-Brunelli, D.; Atvars, T. D. Z.; Joekes, I.; Barbosa, V. C. *J. Appl. Polym. Sci.* **1998**, *64*, 645. (d) Granados, E. G.; González-Benito, J.; Baselga, J.; Dibbern-Brunelli, D.; Atvars, T. D. Z.; Esteban, I.; Piérola, I. F. *J. Appl. Polym. Sci.* **2001**, *80*, 949.
(11) (a) Kramer, E. J.; Green, P.; Palmstrom, J. *Polymer* **1984**, *25*, 473. (b) Wu, S.; Chuang, H.-K.; Han, C. D. *J. Polym. Sci., Part B: Polym. Phys.* **1986**, *24*, 143.
(12) (a) He, Z.; Hammond, G. S.; Weiss, R. G. *Macromolecules* **1992**, *25*, 501−502. (b) He, Z.; Hammond, G. S.; Weiss, R. G. *Macromolecules* **1992**, *25*, 1568.
(13) (a) Schuman, T.; Stepanov, E. V.; Nazarenko, S.; Capaccio, G.; Hiltner, A.; Baer, E. *Macromolecules* **1998**, *31*, 4551. (b) Schuman, T.; Nazarenko, S.; Stepanov, E. V.; Magonov, S. N.; Hiltner, A.; Baer, E. *Polymer* **1999**, *40*, 7373. (c) Tashiro, K.; Gose, N. *Polymer* **2001**, *42*, 8987.
(14) Kim, E.; Kramer, E. J.; Garrett, P. D.; Mendelson, R. A.; Wu, W. C. *Polymer* **1995**, *36*, 2427.
(15) Dongman, C.; Hu, W.; Koberstein, J. T.; Lingelser, J. P.; Gallot, Y. *Macromolecules* **2000**, *33*, 5245.
(16) Talhavini, M.; Atvars, T. D. Z. *J. Photochem. Photobiol. A: Chem.* **1998**, *114*, 65.
(17) Song, L.; Varma, C. A. G. O.; Verhoeven, J. W.; Tanke, H. J. *Biophys. J.* **1997**, *101*, 7683.

MA048873R